

Accuracy of Currently Available Methods in Quantifying Anterior Glenoid Bone Loss: Controversy Regarding Gold Standard—A Systematic Review



Lukas P. E. Verweij, B.Sc., Alexander A. Schuit, B.Sc., Gino M. M. J. Kerkhoffs, M.D., Ph.D., Leendert Blankevoort, Ph.D., Michel P. J. van den Bekerom, M.D., Ph.D., and Derek F. P. van Deurzen, M.D.

Purpose: To determine the accuracy of glenoid bone loss–measuring methods and assess the influence of the imaging modality on the accuracy of the measurement methods. **Methods:** A literature search was performed in the PubMed (MEDLINE), Embase, and Cochrane databases from 1994 to June 11, 2019. The guidelines and algorithm of the Preferred Reporting Items for Systematic Reviews and Meta-analyses (PRISMA) were used. Included for analysis were articles reporting the accuracy of glenoid bone loss–measuring methods in patients with anterior shoulder instability by comparing an index test and a reference test. Furthermore, articles were included if anterior glenoid bone loss was quantified using a ruler during arthroscopy or by measurements on plain radiograph(s), computed tomography (CT) images, or magnetic resonance images in living humans. The risk of bias was determined using the Quality Assessment of Diagnostic Accuracy Studies (QUADAS-2) tool. **Results:** Twenty-one studies were included, showing 17 different methods. Three studies reported on the accuracy of methods performed on 3-dimensional CT. Two studies determined the accuracy of glenoid bone loss–measuring methods performed on radiography by comparing them with methods performed on 3-dimensional CT. Six studies determined the accuracy of methods performed using imaging modalities with an arthroscopic method as the reference. Eight studies reported on the influence of the imaging modality on the accuracy of the methods. There was no consensus regarding the gold standard. Because of the heterogeneity of the data, a quantitative analysis was not feasible. **Conclusions:** Consensus regarding the gold standard in measuring glenoid bone loss is lacking. The use of heterogeneous data and varying methods contributes to differences in the gold standard, and accuracy therefore cannot be determined. **Level of Evidence:** Level IV, systematic review of Level II, III, and IV studies.

See commentary on page 2314

Anterior shoulder dislocation is common in the general population, showing an incidence of 40.4 per 100,000 person-years for men and 15.5 per 100,000 person-years for women.^{1,2} Owing to the advantages of a minimally invasive technique, the arthroscopic Bankart

repair has gained wide popularity and is a frequently performed operative treatment for anterior shoulder instability. Nonoperative treatment shows an alarming recurrent dislocation percentage of 50%, as reported in the literature.³ Of primary anterior dislocations, 13% to 41%

From the Department of Orthopedic Surgery, Amsterdam Movement Sciences, Amsterdam UMC, University of Amsterdam, Amsterdam, The Netherlands (L.P.E.V., A.A.S., G.M.M.J.K., L.B.); Academic Center for Evidence-based Sports medicine (ACES), Amsterdam UMC, Amsterdam, The Netherlands (L.P.E.V., G.M.M.J.K., L.B.); Amsterdam Collaboration for Health and Safety in Sports (ACHSS), International Olympic Committee (IOC) Research Center, Amsterdam UMC, Amsterdam, The Netherlands (L.P.E.V., G.M.M.J.K., L.B.); and Department of Orthopedic Surgery, Onze Lieve Vrouwe Gasthuis, Amsterdam, The Netherlands (M.P.J.v.d.B., D.F.P.v.D.).

The authors report the following potential conflicts of interest or sources of funding: M.P.J.v.d.B. received a research grant from Smith & Nephew and Wright/Tornier, outside the submitted work. D.F.P.v.D. receives research

funding for the orthopaedic department from Wright Medical and receives fellowship funding from Smith & Nephew, outside the submitted work. Full ICMJE author disclosure forms are available for this article online, as supplementary material.

Received October 8, 2019; accepted April 9, 2020.

Address correspondence to Lukas P. E. Verweij, B.Sc., Amsterdam University Medical Center, Meibergdreef 9 1105 AZ, Amsterdam, The Netherlands. E-mail: l.p.verweij@amsterdamumc.nl

© 2020 by the Arthroscopy Association of North America
0749-8063/191212/\$36.00

<https://doi.org/10.1016/j.arthro.2020.04.012>

cause an anterior glenoid rim fracture or chronic erosion of the glenoid rim.⁴⁻⁷ In the case of recurrent shoulder instability, these percentages may even rise to 86%.^{4,6,8,9} These bony lesions have been identified as an important risk factor for failure of conservative treatment and arthroscopic soft-tissue stabilization procedures or revision surgery.¹⁰⁻¹²

Several techniques have been proposed to treat bony insufficiency of the glenoid rim. To date, however, there is no consensus on the cutoff value to decide between bony and soft-tissue procedures to lower the chance of recurrent instability developing.^{13,14} The glenoid can be visualized using imaging modalities such as arthroscopy, plain radiography, computed tomography (CT), and magnetic resonance imaging (MRI). Several quantification methods have been proposed to calculate the amount of bone that is missing in the glenoid.^{15,16} For example, one of the first methods, introduced by Sugaya et al.¹⁷ in 2003, is based on the assumption that the inferior part of the glenoid surface resembles a circle. The missing part of the circle can be used to calculate a percentage. In this example, glenoid bone loss is defined as the proportion of the circle that is not filled by the surface of the inferior part of the glenoid in 2-dimensional (2D) space. In the subsequent years, numerous adaptations of the Sugaya method and new methods have been proposed based on circular and/or linear measurements.

Despite the vast amount of information regarding measuring glenoid bone loss, it is difficult to differentiate between the methods because they are very similar. Previous studies have determined the accuracy of these measurements in cadavers.¹⁸⁻²⁰ However, to assess the clinical applicability of the glenoid bone loss—measuring methods, accuracy in living humans needs to be determined. The validity of a (clinical) test can be subdivided into 2 components: precision and accuracy of the measurement. To achieve high precision, a measurement needs to report the same value repeatedly under the same conditions; this is often referred to as “reliability.” An accurate measurement gives a value that is close to the actual value. If the test is the best available under reasonable conditions, it is considered the gold standard. A recent systematic review by Walter et al.²¹ evaluated the accuracy of glenoid bone loss—measuring methods; however, they did not evaluate the gold standard, and consensus regarding the gold standard may be lacking. Furthermore, cadaveric studies were included, and the Preferred Reporting Items for Systematic Reviews and Meta-analyses (PRISMA) guidelines were not followed²¹; the current study is an update of the literature since January 2018.

The aim of this study was to determine the accuracy of glenoid bone loss—measuring methods and assess the influence of the imaging modality on the accuracy of the measurement methods. We hypothesized that there would be many methods available and that they would

show high accuracy, which would not be influenced by the imaging modality.

Methods

This systematic review focused on the accuracy of currently available methods in quantifying anterior glenoid bone loss. The guidelines and algorithm of the Preferred Reporting Items for Systematic Reviews and Meta-analyses (PRISMA) were used.²² The review protocol (CRD42018083343) has been registered with PROSPERO (<https://www.crd.york.ac.uk/PROSPERO/>).

Literature Search

A literature search was performed in the PubMed (MEDLINE), Embase, and Cochrane databases on June 11, 2019. The search terms for each database are listed in [Appendix Tables 1-3](#) (available at www.arthroscopyjournal.org). The search was performed with the assistance of a clinical librarian and was limited to articles published after 1994. Sugaya et al.¹⁷ introduced the first glenoid bone loss—measuring method that could measure glenoid bone loss in patients with anterior shoulder instability; however, the search was started 10 years in advance to find potential studies on which their study was based. Articles written in the English, Dutch, German, or French language were included.

Study Selection

Articles were included for full-text screening when the abstract mentioned methods to quantify anterior glenoid bone loss using arthroscopy or plain radiographs, CT, or MRI in living humans. Cadaveric studies, animal studies, and studies reporting the quantification of glenoid bone loss for conditions other than an anterior shoulder dislocation were excluded. During full-text screening, articles that evaluated accuracy by means of a comparison between an index test and a reference test using a glenoid bone loss—measuring method and at least one of the earlier reported imaging modalities were included for analysis. Glenoid bone loss was defined as the ratio of the articular glenoid surface that was missing. Studies that were found by cross-referencing and matched the inclusion criteria were included. Studies that did not use the selected imaging modalities or did not report original data were excluded. Titles and abstracts were screened by 2 authors (L.P.E.V. and A.A.S.). Any disagreement was resolved by discussion and consensus. Studies that met the inclusion criteria underwent full-text screening by the same authors (L.P.E.V. and A.A.S.) and were processed in the same manner.

Outcome

The accuracy of the methods by means of a comparison between the index test and a reference test was

extracted as the primary outcome measure. Secondary outcome measures included the use of a gold standard as reference measurement. The homogeneity of the data was evaluated to perform a quantitative analysis or meta-analysis. Correlations of 0.8 to 1.0 were defined as very strong; 0.6 to 0.8, strong; 0.4 to 0.6, moderate; 0.2 to 0.4, weak; and 0.0 to 0.2, very weak. The level of evidence was determined according to Poehling and Jenkins.²³

Risk-of-Bias Analysis

The risk of bias was determined using the Quality Assessment of Diagnostic Accuracy Studies (QUADAS-2) tool.²⁴ This tool consists of 4 domains in which risk of bias is assessed using signaling questions tailored to the review question to determine low, high, or unclear risk: patient selection, index test, reference test, and flow and timing. Moreover, applicability was assessed for patient selection, the index test, and the reference test without the use of signaling questions but according to the review question. If there were any concerns that

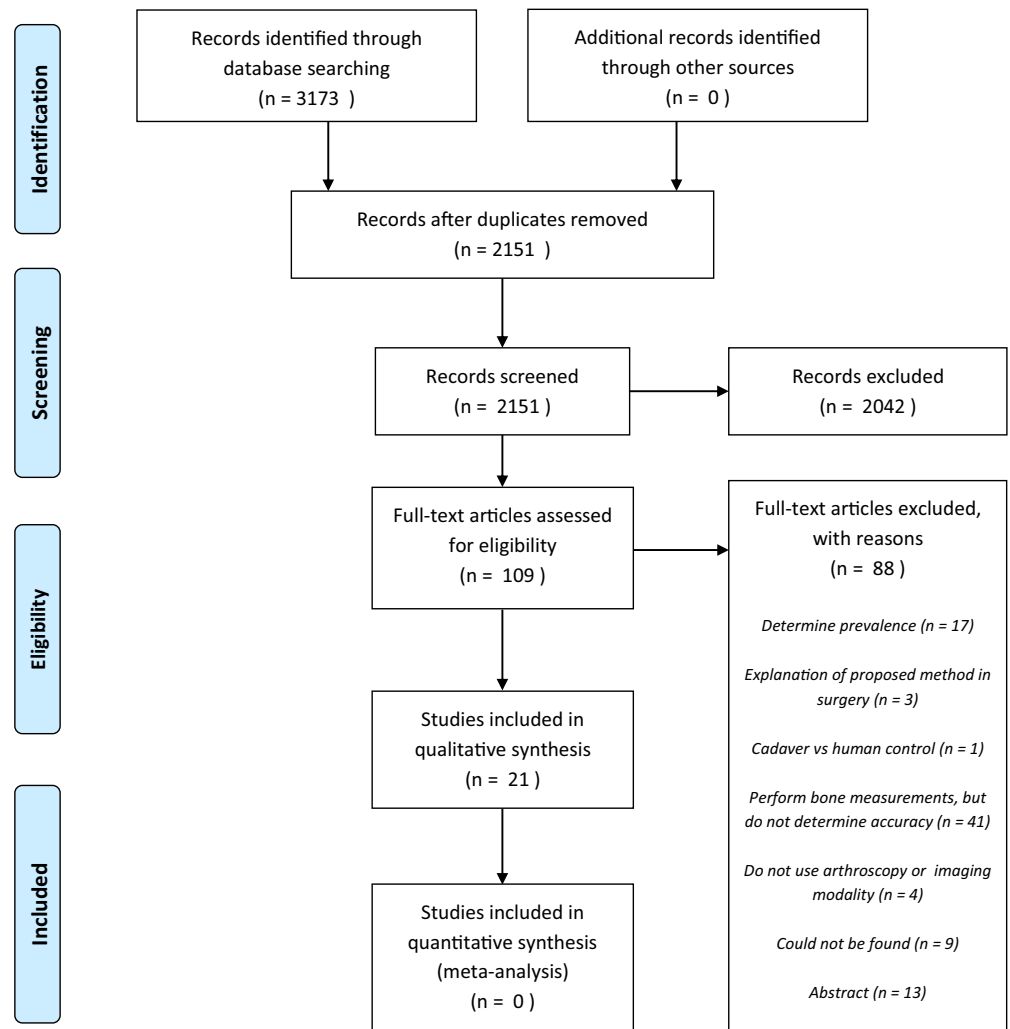
selection, conduction, or interpretation of a domain did not match the review question, it was labeled high risk. The risk-of-bias analysis was performed by 2 authors (L.P.E.V. and A.A.S.). Any disagreement was resolved by discussion and consensus.

Results

Screening and Study Characteristics

The titles and abstracts of 3,173 articles resulting from the initial search were screened, 109 articles underwent full-text screening, and 21 studies were included for analysis (Fig 1). Cross-referencing did not result in additional studies. The sample size per study ranged from 7 to 100 shoulders. A total of 673 shoulders were examined. The studies originated from the United States,²⁵⁻³² Canada,³³⁻³⁵ China,³⁶⁻³⁸ Italy,^{39,40} Japan,⁴¹ Brazil,^{42,43} Germany,⁴⁴ and France.⁴⁵ The included studies were published between December 2007 and October 2019.

Fig 1. Flow diagram.



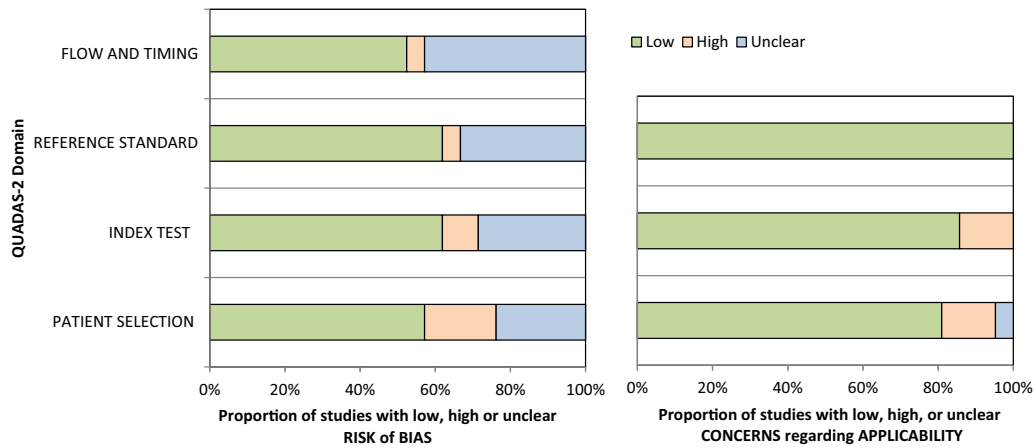


Fig 2. Quality Assessment of Diagnostic Accuracy Studies (QUADAS-2) risk-of-bias analysis: proportions of low, high, or unclear risk of bias and low, high, or unclear concerns regarding applicability.

Risk-of-Bias Analysis

Risk-of-bias analysis showed a low risk in less than 60% of studies in the flow-and-timing domain, less than 70% in the reference-standard and index-test domains, and less than 60% in the patient-selection domain (Fig 2). For analysis of concerns regarding applicability, more than 80% of studies had a low risk in the index-test and patient-selection domains and 100% had a low risk in the reference-test domain (Fig 2). Many studies did not report whether the tests were blinded or how much time elapsed between the index and reference tests. That is why these domains

frequently scored an unclear risk. The quality assessment of the individual studies can be found in Table 1.

Characteristics of Glenoid Bone Loss—Measuring Methods

Seventeen different measurement methods were used in the included articles (Table 2). All the methods calculated the ratio of the glenoid surface that was missing in 2D space. Thirteen methods were based on unilateral measurement of the glenoid, whereas 4 were based on bilateral measurements. Measurements were performed using the glenoid

Table 1. Risk-of-Bias and Applicability Analyses of QUADAS-2 Tool for Each Study

Study	Risk of Bias				Applicability Concerns		
	Patient Selection	Index Test	Reference Standard	Flow and Timing	Patient Selection	Index Test	Reference Standard
Bakshi et al. ²⁵	+	?	?	+	+	+	+
Bakshi et al. ²⁶	+	+	+	?	+	+	+
Chuang et al. ²⁷	-	?	?	?	+	+	+
Giles et al. ³³	?	+	-	+	-	+	+
Griffith et al. ³⁶	+	-	+	?	+	+	+
Gyftopoulos et al. ²⁸	?	+	+	?	+	-	+
Gyftopoulos et al. ²⁹	+	+	+	?	+	-	+
Lacheta et al. ⁴⁴	+	+	+	+	+	+	+
Lansdown et al. ³²	+	?	?	+	?	+	+
Lee et al. ³⁷	?	+	+	?	+	-	+
Magarelli et al. ³⁹	+	+	+	+	+	+	+
Miyatake et al. ⁴¹	+	?	?	-	+	+	+
Murachovsky et al. ⁴²	+	+	?	+	+	+	+
Pansard et al. ⁴⁵	?	+	+	?	+	+	+
Parada et al. ³⁰	-	+	+	+	+	+	+
Rouleau et al. ³⁴	?	?	?	+	+	+	+
Souza et al. ⁴³	+	-	+	?	+	+	+
Stecco et al. ⁴⁰	+	?	?	+	+	+	+
Stillwater et al. ³⁵	+	+	+	+	+	+	+
Tian et al. ³⁸	-	+	+	+	-	+	+
Vopat et al. ³¹	-	+	+	?	-	+	+

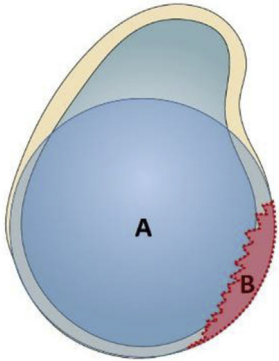
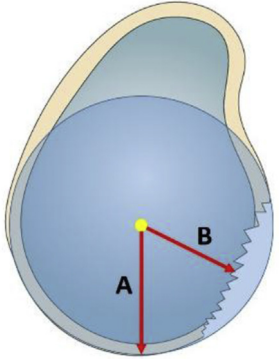
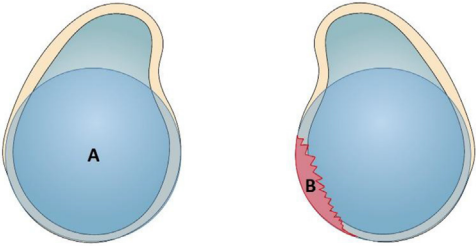
NOTE. A plus sign indicates low risk; minus sign, high risk; and question mark, unclear risk. QUADAS-2, Quality Assessment of Diagnostic Accuracy Studies.

Table 2. Glenoid Bone Loss—Measuring Methods Used in Articles Included in This Study

Method	Unilateral or Bilateral	Explanation	Image
Bernageau-view method ^{42,45}	Bilateral	With the patient's arm in abduction, bilateral radiographic Bernageau glenoid profile views are acquired. The diameter of the pathologic shoulder (A) is divided by the diameter of the healthy shoulder (B) to calculate the percentage using the following expression: $[1 - (A/B)] \times 100$.	
Best-fit circle using glenoid fragment ^{26,45}	Unilateral	On a sagittal view, a circle is placed on the glenoid that best fits the 3- to 9-o'clock inferior contour and the area (A) is determined. The osseous fragment is located, and the area (B) is determined as well. The percentage is calculated using the following expression: $B/A \times 100$.	
Best-fit circle using missing area ^{31,34,37,43}	Unilateral	On a sagittal view, a circle is placed on the glenoid that best fits the 3- to 9-o'clock inferior contour and the area (A) is determined. The missing area of the circle (B) is determined as well. The percentage is calculated using the following expression: $B/A \times 100$.	

(continued)

Table 2. Continued

Method	Unilateral or Bilateral	Explanation	Image
Best-fit circle using point selection ³⁰	Unilateral	On a sagittal view, a circle is placed on the glenoid that best fits the 3- to 9-o'clock inferior contour and the area (A) is determined. The image is enlarged to manually trace the rim by making point selections, and the area (B) of bone loss is determined. The percentage is calculated using the following expression: $B/A \times 100$.	
Best-fit circle using ratio method ^{26,34}	Unilateral	On a sagittal view, a circle is placed on the glenoid that best fits the 3- to 9-o'clock inferior contour and the radius (A) of the circle is determined. Furthermore, the distance between the anterior glenoid and the center of the circle (B) is determined. The ratio is calculated according to the following expression: B/A .	
Best-fit circle using Pico method ^{25,26,32,39,40}	Bilateral	On a sagittal view of the healthy shoulder (left), a circle is placed on the glenoid that best fits the 3- to 9-o'clock inferior contour, and the area (A) is determined. The circle is then superimposed onto the injured shoulder (right). The area of bone loss (B) is determined. The percentage is calculated using the following expression: $B/A \times 100$.	

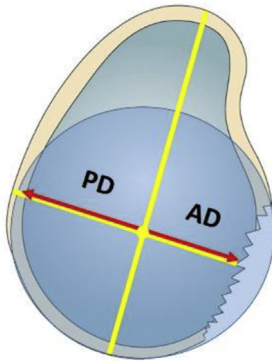
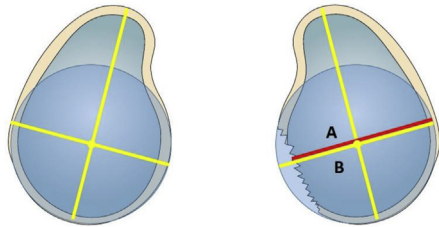
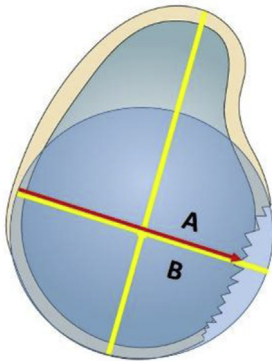
(continued)

Table 2. Continued

Method	Unilateral or Bilateral	Explanation	Image
Best-fit circle using clock method ³⁴	Unilateral	On a sagittal view, a circle is placed on the glenoid that best fits the 3- to 9-o'clock inferior contour. The glenoid clock method uses angles to determine a "beginning time" (A), which is the starting point of the measurement, and an "ending time" (B). The amount of time between the beginning and ending times resembles the glenoid defect and can be linked to a percentage through an algebraic equation.	
Best-fit circle using circle-line method ³⁰	Unilateral	On a sagittal view, a circle is placed on the glenoid that best fits the 3- to 9-o'clock inferior contour, and the area (A) is determined. A straight line best following the glenoid bone loss is drawn. Furthermore, a line perpendicular to the previous straight line is drawn. Algebraic geometry can be used to determine the area (B) of bone loss. The percentage is calculated using the following expression: $B/A \times 100$.	

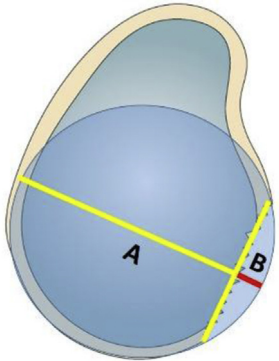
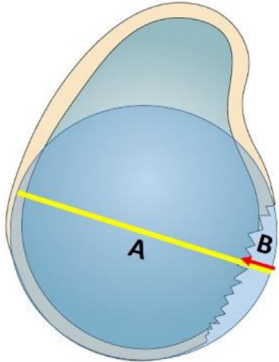
(continued)

Table 2. Continued

Method	Unilateral or Bilateral	Explanation	Image
Best-fit circle using bare spot ^{25,26}	Unilateral	On a sagittal view, a longitudinal axis is drawn from the supraglenoid tubercle through the inferior aspect of the inferior glenoid rim. Furthermore, a straight line perpendicular to the longitudinal axis is drawn at the widest point of the glenoid. The intersection of these lines resembles the bare spot and is used to draw a circle. The percentage of glenoid bone loss is calculated with the posterior distance (PD) and anterior distance (AD) using the following expression: $[(PD - AD)/(2 \times PD)] \times 100$.	
Best-fit circle using glenoid index ^{27,41}	Bilateral	On a sagittal view of the healthy shoulder (left), a straight line is drawn from the most superior point to the most inferior point of the glenoid. Furthermore, a straight perpendicular line is drawn at the widest point of the glenoid. The intersection of these lines is used as a geometric center to draw a circle. By use of the data of the healthy shoulder, the geometric center of the healthy shoulder can be superimposed onto the injured shoulder (right) to determine the width (A) of the injured glenoid. Moreover, the expected width (B) is determined using the circle. The ratio is calculated according to the following expression: A/B .	
Best-fit circle using circle diameter I ^{35,37}	Unilateral	On a sagittal view, a longitudinal axis is drawn from the supraglenoid tubercle through the inferior aspect of the inferior glenoid rim. Furthermore, guided by the longitudinal axis, a circle is placed on the glenoid that best fits the 3- to 9-o'clock inferior contour. A straight line, perpendicular to the previous line, is drawn through the center of the circle until the defect is reached (A). The diameter of the circle (B) is determined as well. The percentage of glenoid bone loss is calculated using the following expression: $(B - A/B) \times 100$.	

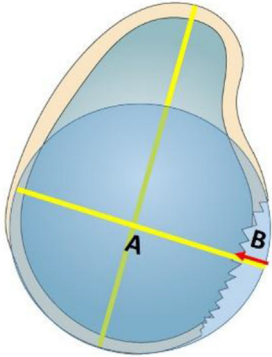
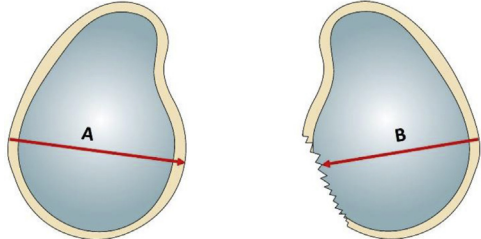
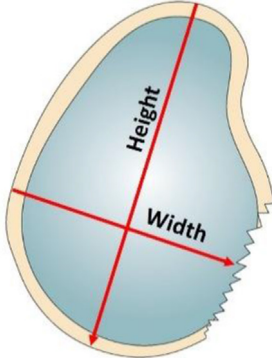
(continued)

Table 2. Continued

Method	Unilateral or Bilateral	Explanation	Image
Best-fit circle using circle diameter 2 ³⁸	Unilateral	On a sagittal view, a circle is placed on the glenoid that best fits the 3- to 9-o'clock inferior contour. A line is drawn from the posterior side to the anterior side of the circle to determine the diameter (A); this represents an intact glenoid. A second straight line is drawn following the glenoid defect; this will enable measurement of the glenoid defect (B). The percentage of glenoid bone loss is calculated using the following expression: $(B/A) \times 100$.	
Best-fit circle using circle diameter 3 ^{28,44}	Unilateral	On a sagittal view, a circle is placed on the glenoid that best fits the 3- to 9-o'clock inferior contour. A line is drawn from the posterior side to the anterior side of the circle to determine the diameter (A); this represents an intact glenoid. Furthermore, a line is drawn from the anterior margin of the circle to the glenoid defect (B). The percentage is calculated using the following expression: $(B/A) \times 100$.	

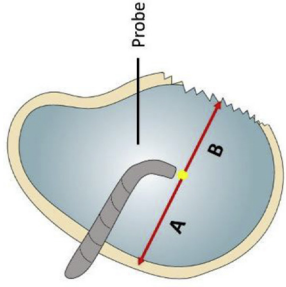
(continued)

Table 2. Continued

Method	Unilateral or Bilateral	Explanation	Image
Best-fit circle using circle diameter ^{4,29}	Unilateral	On a sagittal view, a straight line is drawn from the superior glenoid tubercle to the inferior margin of the glenoid; this line is used to place a circle on the glenoid that best fits the 3- to 9-o'clock inferior contour. A line is drawn from the posterior side to the anterior side of the circle to determine the diameter (A); this represents an intact glenoid. Furthermore, a line is drawn from the anterior margin of the circle to the glenoid defect (B). The percentage is calculated using the following expression: $(B/A) \times 100$.	
Bilateral AP distance ^{36,42}	Bilateral	On a sagittal view, the diameter at the widest point of the glenoid is determined for the healthy shoulder (A, left glenoid). Furthermore, the diameter of the injured shoulder (B, right glenoid) is determined to calculate the percentage using the following expression: $[1 - (B/A)] \times 100$.	
Glenoid height-width correlation ³³	Unilateral	On the basis of the correlation between glenoid height and glenoid width, formulas were created that are sex specific. The formula for male patients is $\text{Width} = \text{One-third height} + 15 \text{ mm}$. The formula for female patients is $\text{Width} = \text{One-third height} + 13 \text{ mm}$. The expected glenoid width can be calculated with these formulas, and the percentage is calculated according to the following expression: $[(1 - \text{Glenoid width})/\text{Expected glenoid width}] \times 100$.	

(continued)

Table 2. Continued

Method	Unilateral or Bilateral	Explanation	Image
Bare-spot method ^{2,6-29,36,37,41,43}	Unilateral	During arthroscopy, the distance from the posterior glenoid to the bare spot (A) is measured with a probe, as is the distance between the anterior glenoid and the bare spot (B). The percentage is calculated according to the following expression: $[B / (A \times 2)] \times 100$.	

AP, anterior-posterior.

surface (sagittal en face view of the glenoid) in 16 methods and using the glenoid rim (sagittal view) in 1 method. Eleven methods used a distance that was divided by a reference distance, 5 methods used a surface that was divided by a reference surface, and 1 method used the position of the defect to quantify glenoid bone loss (Table 2). The methods were used on 6 different imaging modalities (Table 3).

Accuracy of Methods Performed on 3-Dimensional CT

Three studies reported on the accuracy of the methods on 3-dimensional (3D) CT (Table 4).^{25,30,34} Bakshi et al.²⁵ reported an overestimation ($P < .001$) with the linear-based best-fit circle (bare spot) (mean, $17.5\% \pm 9.7\%$) compared with the circular-based best-fit circle (Pico method) (mean, $12.8\% \pm 8.0\%$) on 3D CT. Parada et al.³⁰ did not show a difference between the circular- and linear-based best-fit circle (circle-line method) and the circular-based best-fit circle (point selection) in 7 patients whereas they found a difference in 1 patient with 25% bone loss ($P = .005$). Rouleau et al.³⁴ showed a strong correlation between the circular-based best-fit circle (clock method), best-fit circle using the missing area ($r = 0.793, P < .001$), and best-fit circle using the ratio method ($r = 0.717, P < .001$).

Accuracy of Methods Performed on Radiography Compared With 3D CT

Two studies compared the Bernageau-view method with methods performed on 3D CT.^{42,45} Murachovsky et al.⁴² reported no difference between the Bernageau-view method (mean, 24.10 ± 4.12 mm) and the bilateral anterior-posterior distance determined on 3D CT (mean, 23.42 ± 4.55 mm; $P = .513$). Pansard et al.⁴⁵ showed a moderate to strong correlation between the Bernageau view (mean, $8.5\% \pm 4.5\%$) and best-fit circle (glenoid fragment) (mean, $9.0\% \pm 5.9\%$), from $r = 0.56 (P < .001)$ to $r = 0.8 (P < .001)$.

Accuracy of Methods Performed on Imaging Modalities Compared With Bare-Spot Method

Six studies compared methods performed on imaging modalities with the bare-spot method as the reference (Table 4).^{27-29,36,37,43} Chuang et al.²⁷ showed that the linear- and circular-based best-fit circle (glenoid index) determined on 3D CT accurately predicted the same preferred treatment as the bare-spot method (96% agreement, $P < .001$). Griffith et al.³⁶ found that the linear-based bilateral anterior-posterior distance determined on 2D CT (mean, $11.0\% \pm 8.1\%$) did not show a difference compared with the bare-spot method (mean, $12.3\% \pm 8.8\%$). Gyftopoulos et al.²⁸ reported that the circular- and linear-based best-fit circle (circle diameter 3) (mean, 12.6%) determined on 3D MRI did not show

Table 3. Overview of Modalities Used to Perform Glenoid Bone Loss—Measuring Methods

Modality	Explanation
Arthroscopy	During minimally invasive surgery, a probe can be inserted through one of the incisions to measure distances and perform the bare-spot method.
Radiography	Shoulder radiography is performed in the Bernageau position, in which the arm is elevated and pressed against the plate and the x-ray tube is placed at an angle of 30°. This view produces a clear image of the glenoid rim.
2D CT	A standard CT scan of the shoulder is performed, in which many radiographic measurements are combined to produce slices of the scanned object. CT can be viewed in the axial, coronal, or sagittal plane. Typically, the scapula is viewed in the sagittal plane to produce a view of the glenoid surface and perform the measuring methods.
3D CT	By combining the 3 planes of the standard (2D) CT scan and a segmentation software tool, a 3D image of the scapula is created. This image can be viewed from any direction in 3D space. A sagittal view of the scapula produces a clear view of the glenoid surface to perform the measuring methods.
2D MRI	An MRI scan of the shoulder is performed. Depending on the settings during the scan, the MRI can be viewed in the axial, coronal, or sagittal plane. Typically, the scapula is viewed in the sagittal sequence to produce a view of the glenoid surface and perform the measuring methods.
3D MRI	By combining the axial, coronal, and sagittal planes of the (2D) MRI scan and a segmentation software tool, a 3D image of the scapula is created. This image can be viewed from any direction in 3D space. A sagittal view of the scapula produces a clear view of the glenoid surface to perform the measuring methods.

CT, computed tomography; MRI, magnetic resonance imaging; 3D, 3-dimensional; 2D, 2-dimensional.

a difference compared with the bare-spot method (mean, 12.7%; $P = .767$). Furthermore, they reported that the circular- and linear-based best-fit circle (circle diameter 4) (mean, 16.4% \pm 12.5%) determined on 2D MRI did not show a difference compared with the bare-spot method (mean, 16.25% \pm 12.5%; $P = .893$).²⁹ Lee et al.³⁷ reported a very strong correlation between the circular-based best-fit circle (missing area) determined on 2D MRI ($r = 0.84$, $P < .001$) and circular- and linear-based best-fit circle (circle diameter 1) determined on 2D CT ($r = 0.91$, $P < .001$) compared with the bare-spot method. Souza et al.⁴³ reported a strong correlation between the best-fit circle (missing area) determined on 2D MRI and the bare-spot method for observer 1 ($r = 0.76$), as well as a moderate correlation for observer 2 ($r = 0.69$).

Two studies compared the bare-spot method with imaging modalities as the reference (Table 4).^{26,41} Bakshi et al.²⁶ reported an overestimation with the bare-spot method (18.13% \pm 11.81%) compared with the best-fit circle using the glenoid fragment (12.15% \pm 8.50%, $P = .005$), best-fit circle using the Pico method (12.77% \pm 8.17%, $P = .002$), best-fit circle using the bare spot (12.44% \pm 10.68%, $P = .001$), and best-fit circle using the ratio method (9.50% \pm 8.74%, $P < .001$) performed on 3D CT. Miyatake et al.⁴¹ reported a strong correlation ($r = 0.63$, $P < .001$) between the bare-spot method (mean, 15.1% \pm 10.0%) and best-fit circle (glenoid index) (mean, 13.6% \pm 9.3%).

Influence of Imaging Modality on Accuracy

Eight studies compared imaging modalities using the same method (Table 4).^{31-33,35,38-40,44} Giles et al.³³ reported a very strong correlation for the glenoid height–width correlation determined on 3D CT versus 3D MRI ($r = 0.9$, $P < .001$) and a very strong sex-specific correlation for male patients ($r = 0.811$, $P <$

.001), as well as a strong correlation for female patients ($r = 0.747$, $P < .001$). Lacheta et al.⁴⁴ reported an overestimation of the best-fit circle (circle diameter 3) determined on 2D CT compared with 3D CT in both the first measurement (mean first measurement, 7.3% \pm 3.0% vs 6.1% \pm 2.7%; $P < .001$) and second measurement (mean second measurement, 7.1% \pm 3.1% vs 6.0% \pm 7.6%; $P = .003$). Lansdown et al.³² reported that the best-fit circle (Pico method) determined on 3D MRI and 3D CT showed a less than 2% difference in 88% of the measurements. This was defined as not clinically relevant. Magarelli et al.³⁹ reported that the best-fit circle (Pico method) determined on 2D CT and 3D CT did not show a clinically relevant difference (0.62%, with a clinically relevant difference defined as >5%). Stecco et al.⁴⁰ reported that the best-fit circle (Pico method) determined on 2D MRI (mean, 4.38%) and 2D CT (mean, 4.34%) did not show a difference. Stillwater et al.³⁵ reported that the best-fit circle (circle diameter 1) calculated on 3D MRI and 3D CT did not show a difference ($P = .34$). Tian et al.³⁸ reported that the best-fit circle (circle diameter 2) calculated on 2D MRI (mean, 10.48% \pm 8.71%) and 2D CT (mean, 10.96% \pm 9.00%) showed no difference ($P = .288$). Vopat et al.³¹ reported that the best-fit circle (missing area) determined on 3D MRI and 3D CT did not show a difference ($P = .852$ for automated segmentation and $P = .801$ for manual segmentation).

Gold Standard

Bakshi et al.,²⁵ Lansdown et al.,³² Pansard et al.⁴⁵ and Vopat et al.³¹ considered 3D CT the gold standard to quantify glenoid bone loss but did not mention anything about the gold standard of glenoid bone loss—measuring methods. Griffith et al.³⁶ reported that they used arthroscopic assessment as the gold standard but mentioned that it was not the ideal gold standard.

Table 4. Accuracy of Glenoid Bone Loss—Measuring Methods: Study Characteristics and Outcomes Reported in Included Studies

Authors (Year)/ Study Design	Level of Evidence	Sample Size	Index Test Modality	Index Test Measuring Method	Outcome	RS Modality	RS Measuring Method
Bakshi et al. ²⁵ (2018)/ retrospective	III	28: 23 M and 5 F	3D CT	Best-fit circle (bare spot)	The paired 2-tailed <i>t</i> test showed a significant difference ($P < .001$) between the best-fit circle using the bare spot (mean, $17.5\% \pm 9.7\%$) and best-fit circle using the Pico method (mean, $12.8\% \pm 8.0\%$).	3D CT (GS)	Best-fit circle (Pico method)
Bakshi et al. ²⁶ (2015)/ retrospective	IV	20: 15 M and 5 F	Arthroscopy	Bare-spot method	The paired 2-tailed <i>t</i> test showed significant overestimation with the bare-spot method ($18.13\% \pm 11.81\%$) compared with the best-fit circle using the glenoid fragment ($12.15\% \pm 8.50\%$, $P = .005$), best-fit circle using the Pico method ($12.77\% \pm 8.17\%$, $P = .002$), best-fit circle using the bare spot ($12.44\% \pm 10.68\%$, $P = .001$), and best-fit circle using the ratio method ($9.50\% \pm 8.74\%$, $P < .001$).	3D CT (not true GS*)	Best-fit circle using glenoid fragment Best-fit circle using Pico method Best-fit circle using bare spot Best-fit circle using ratio method
Chuang et al. ²⁷ (2008)/ retrospective	III	25	3D CT	Best-fit circle (glenoid index)	The Fisher exact test showed that the best-fit circle (glenoid index) accurately predicted the same preferred treatment in 96% of patients (24 of 25) compared with arthroscopy ($P < .001$).	Arthroscopy (not true GS*)	Bare-spot method
Giles et al. ³³ (2015)/ retrospective	III	90: 60 M and 30 F	3D CT	Glenoid height— width correlation	The Pearson correlation coefficient (<i>r</i>) showed an overall correlation between 3D CT and MRI of 0.900 ($P < .001$) and sex-specific correlations of 0.811 ($P < .001$) for male patients and 0.747 ($P < .001$) for female patients.	3D MRI (not true GS*)	Glenoid height— width correlation
Griffith et al. ³⁶ (2007)/ prospective	II	55: 45 M and 10 F	2D CT	Bilateral AP distance	The Student <i>t</i> test did not find a significant difference ($P = .17$) between CT (mean, $11.0\% \pm 8.1\%$) and arthroscopy (mean, $12.3\% \pm 8.8\%$), and the Pearson correlation (<i>r</i>) was 0.79 ($P < .001$).	Arthroscopy (GS)	Bare-spot method
Gyftopoulos et al. ²⁸ (2014)/ retrospective	III	15: 13 M and 2 F	3D MRI	Best-fit circle (circle diameter 3)	The Wilcoxon test showed no significant difference between the best-fit circle (circle diameter 3) (mean, 12.6%) and bare-spot method (mean, 12.7% ; $P = .767$).	Arthroscopy (GS)	Bare-spot method
Gyftopoulos et al. ²⁹ (2013)/ retrospective	III	12	2D MRI	Best-fit circle (circle diameter 4)	The Wilcoxon test showed no significant difference between the best-fit circle (circle diameter 4) (mean, $16.4\% \pm 12.5\%$) and bare-spot method (mean, $16.25\% \pm 12.5\%$; $P = .893$).	Arthroscopy (RS)	Bare-spot method

(continued)

Table 4. Continued

Authors (Year)/ Study Design	Level of Evidence	Sample Size	Index Test Modality	Index Test Measuring Method	Outcome	RS Modality	RS Measuring Method
Lacheta et al. ⁴⁴ (2019)/ retrospective	III	26	2D CT	Best-fit circle (circle diameter 3)	The Mann-Whitney <i>U</i> test showed a significant overestimation with 2D CT (mean first measurement, 7.3% ± 3.0%; mean second measurement, 7.1% ± 3.1%) compared with 3D CT (mean first measurement, 6.1% ± 2.7%; mean second measurement, 6.0% ± 7.6%) at the first (<i>P</i> < .001) and second (<i>P</i> = .003) measurements.	3D CT (RS)	Best-fit circle (circle diameter 3)
Lansdown et al. ³² (2019)/ retrospective	III	16: 11 M and 5 F	3D MRI	Best-fit circle (Pico method)	The Bland-Altman plot showed a <2% difference between 3D MRI and 3D CT in 88% of the measurements. This was defined as not clinically relevant.	3D CT (GS)	Best-fit circle (Pico method)
Lee et al. ³⁷ (2013)/ retrospective	III	65	2D MRI 2D CT	Best-fit circle using missing area Best-fit circle using circle diameter 1	MRI showed Pearson correlations (<i>r</i>) of 0.84 (95% CI, 0.81-0.87; <i>P</i> < .001) between the best-fit circle using diameter 1 and the bare-spot method and 0.81 (95% CI, 0.78-0.83; <i>P</i> < .001) between the best-fit circle using the missing area and the bare-spot method. CT showed a Pearson correlation (<i>r</i>) of 0.91 (95% CI, 0.85-0.95; <i>P</i> < .001) between the best-fit circle using circle diameter 1 and the bare-spot method.	Arthroscopy (RS)	Bare-spot method
Magarelli et al. ³⁹ (2012)/ prospective	II	100: 83 M and 17 F	2D CT	Best-fit circle (Pico method)	The Bland-Altman plot showed a mean difference of 0.62% between 2D CT and 3D CT (95% CI, 0.29%-0.92%). A clinically important difference was stated at >5%.	3D CT (not true GS*)	Best-fit circle (Pico method)
Miyatake et al. ⁴¹ (2014)/ prospective	II	35	Arthroscopy	Bare-spot method	A Pearson correlation coefficient (<i>r</i>) of 0.63 (<i>P</i> < .001) was noted between the bare-spot method (mean, 15.1% ± 10.0%) and best-fit circle (glenoid index) (mean, 13.6% ± 9.3%).	3D CT (RS)	Best-fit circle (glenoid index)
Murachovsky et al. ⁴² (2012)/ prospective	III	10: 9 M and 1 F	Radiography (Bernageau)	Bernageau-view method	The Wilcoxon test showed no significant difference between the Bernageau-view method (mean, 24.10 ± 4.12 mm) and bilateral AP distance (mean, 23.42 ± 4.55 mm; <i>P</i> = .513).	3D CT (RS)	Bilateral AP distance
Pansard et al. ⁴⁵ (2013)/ retrospective	III	20: 12 M and 8 F	Radiography (Bernageau)	Bernageau-view method	The Spearman rank correlation coefficient (<i>r</i>) between the Bernageau-view method (mean, 8.5% ± 4.5%) and best-fit circle (glenoid fragment) (mean, 9.0% ± 5.9%) was between 0.56 (<i>P</i> < .001) and 0.8 (<i>P</i> < .001), with an intraclass correlation coefficient (<i>ρ</i>) between 0.82 (<i>P</i> < .001) and 0.86 (<i>P</i> < .001).	3D CT (GS)	Best-fit circle (glenoid fragment)

(continued)

Table 4. Continued

Authors (Year)/ Study Design	Level of Evidence	Sample Size	Index Test Modality	Index Test Measuring Method	Outcome	RS Modality	RS Measuring Method
Parada et al. ³⁰ (2018)/ retrospective	III	8	3D CT	Best-fit circle (circle-line method)	Tukey post hoc honestly significant difference analysis did not show a significant difference in 7 patients (6%, 11%, 11%, 15%, 16%, 20%, and 33% bone loss) between the best-fit circle using the circle-line method and best-fit circle using point selection and showed a significant difference in the patients with 25% glenoid bone loss ($P = .005$).	3D CT (not true GS*)	Best-fit circle (point selection)
Rouleau et al. ³⁴ (2017)/ retrospective	III	34: 29 M and 3 F	3D CT	Best-fit circle (clock method)	The Pearson correlation coefficient (r) showed a strong correlation between the best-fit circle using the clock method and the best-fit circle using the missing area (0.793, $P < .001$), as well as best-fit circle using the ratio method (0.717, $P < .001$).	3D CT (not true GS*)	Best-fit circle using missing area Best-fit circle using ratio method
Souza et al. ⁴³ (2014)/ prospective	II	36: 29 M and 7 F	2D MRI	Best-fit circle (missing area)	The Pearson correlation coefficient (r) showed a correlation between the best-fit circle (missing area) and bare-spot method (mean, 23% \pm 7.6%) for observer 1 (mean, 21% \pm 7.8%; $r = 0.76$; strong correlation) and observer 2 (mean, 20% \pm 6.8%; $r = 0.69$; moderate correlation).	Arthroscopy (GS)	Bare-spot method
Stecco et al. ⁴⁰ (2013)/ prospective	II	23: 22 M and 1 F	2D MRI	Best-fit circle (Pico method)	Coefficients of variance analysis showed no significant differences between 2D MRI (mean, 4.38%) and 2D CT (mean, 4.34%).	2D CT (GS)	Best-fit circle (Pico method)
Stillwater et al. ³⁵ (2017)/ prospective	II	7	3D MRI	Best-fit circle (circle diameter 1)	The paired t test did not show a significant difference between 3D MRI and 3D CT ($P = .34$).	3D CT (GS)	Best-fit circle (circle diameter 1)
Tian et al. ³⁸ (2012)/ prospective	II	40	2D MRI	Best-fit circle (circle diameter 2)	The double-sided paired-sample t test showed no significant difference ($P = .288$) and the Spearman rank coefficient (r) showed a high correlation of 0.912 ($P < .001$) between 2D MRI (mean, 10.48% \pm 8.71%) and 2D CT (mean, 10.96% \pm 9.00%).	2D CT (RS)	Best-fit circle (circle diameter 2)
Vopat et al. ³¹ (2018)/ prospective	III	8: 6 M and 2 F	3D MRI	Best-fit circle (missing area)	The paired Student t test showed no significant difference between 3D MRI and 3D CT ($P = .852$ for automated segmentation and $P = .801$ for manual segmentation).	3D CT (GS)	Best-fit circle (missing area)

AP, anterior-posterior; CI, confidence interval; CT, computed tomography; F, female; GS, study used reference test as gold standard; M, male; MRI, magnetic resonance imaging; RS, study used modality as reference standard and did not mention anything about it being gold standard; 3D, 3-dimensional; 2D, 2-dimensional.

*The study used the modality as the reference standard and mentioned that this was not the true gold standard.

They did not mention anything about the gold standard of glenoid bone loss—measuring methods. Gyftopoulos et al.²⁸ reported that 3D CT is the current imaging gold standard and that the bare-spot method is the gold standard at their institution. Lacheta et al.⁴⁴ and Stecco et al.⁴⁰ considered CT the current standard to quantify glenoid bone loss but did not mention anything about the gold standard of glenoid bone loss—measuring methods. Parada et al.³⁰ reported that a true gold standard does not exist but that the best-fit circle (point selection) method is closest to an actual gold standard. Souza et al.⁴³ reported that arthroscopic findings are the gold standard for the measurement of glenoid bone loss but mentioned that they were not the ideal gold standard. Moreover, they noted that CT is the gold standard for preoperative evaluation of glenoid bone loss but did not mention anything about the gold standard of glenoid bone loss—measuring methods. Tian et al.³⁸ reported that some authors consider CT the gold standard, but they did not report anything about what they consider the gold standard. Of the remaining studies, some reported that there is no gold standard^{26,27,35,39} whereas others did not mention anything about a gold standard.^{29,34,37,41,42}

Statistical Analysis

Owing to the heterogeneity of the reported data, a meta-analysis or quantitative analysis was not feasible.

Discussion

The most important finding was that the accuracy of the glenoid bone loss—measuring methods seems to be good. However, many different imaging modalities and measurement methods are used. There is no consensus regarding a gold standard, which raises the question of whether a gold standard exists for glenoid bone loss measurement. Moreover, if the included studies have been performed without an appropriate gold standard, it can be questioned whether the accuracy can be determined at all.

In total, 17 different methods were described in the included studies, based on either unilateral or bilateral measurements. These methods use circular and/or linear measurements and calculate a ratio. In most studies, this ratio is reported as a percentage. Three studies determined the accuracy of these methods on 3D CT. One study found an overestimation of the best-fit circle using the bare spot compared with the best-fit circle using the Pico method. The other studies did not show a difference and a strong correlation between the methods. Two studies compared the Bernageau-view method with methods performed on 3D CT. They found a difference and a moderate to strong correlation. Six studies compared methods performed on imaging modalities with the bare-spot method; they did not show a (clinically relevant) difference and a strong

correlation. Two studies compared the bare-spot method with methods performed on imaging modalities. One showed an overestimation of the bare-spot method compared with the best-fit circle using the glenoid fragment, as well as the best-fit circle using the Pico method, best-fit circle using the bare spot, and best-fit circle using the ratio method. The other showed a strong correlation between the bare-spot method and best-fit circle (glenoid index).

Eight studies compared imaging modalities using the same method. Two studies compared 2D CT with 3D CT. One study showed an overestimation of methods performed on 2D CT compared with 3D CT, whereas the other study showed no clinically important difference. Four studies compared 3D MRI with 3D CT. They did not show a (clinically important) difference for the best-fit circle using the missing area, best-fit circle using the Pico method, and best-fit circle using circle diameter 1. Furthermore, 1 study showed a very strong correlation and a strong to very strong sex-specific correlation for the glenoid height—width correlation. Two studies compared 2D MRI and 2D CT and did not show a difference for the best-fit circle using the Pico method and the best-fit circle using circle diameter 2.

From a clinical viewpoint, the described methods are used to assess the risk of recurrence by finding the percentage or ratio of glenoid bone deficiency.⁴⁶ However, glenoid bone loss is not the only factor that determines the stability of the shoulder. Other important factors are the presence of a Hill-Sachs lesion, neuromuscular control, and muscle strength and laxity.^{6,47,48} By taking only one of these factors into account, finding a cutoff value may be very difficult. Furthermore, this may partly explain why there is no consensus regarding the methods.

Achieving consensus regarding these methods might be hampered by several factors.⁴⁹ First, the methods are 2D measurement methods and are commonly applied to 3D segmentation models, such as 3D CT and 3D MRI. They measure the same glenoid surface as 2D CT and 2D MRI. The way in which the methods acquire the sagittal view differs. This could partly explain the correlation between the 2D and 3D imaging modalities. Second, in the 3D aspect, glenoid bone loss influences glenoid version and changes the morphology.⁵⁰ It is impossible to account for glenoid version or concavity if a 2D measurement method is used.^{51,52} Third, the standardization and accuracy of glenoid bone loss measurements can be questioned because they are influenced by scapular tilt and best-fit circle placement.⁵³ Fourth, the location of bone loss is not always at the same position, and glenoid rims may have variable contours.^{54,55} Fifth, arthroscopy uses the bare spot to determine glenoid bone loss, and it has been reported that this is not always visible or centered in the inferior glenoid.^{41,56,57} If these methods are not suited to

objectively measure glenoid bone loss or determine recurrence risk, controversy is created.

An example of a contributor to controversy is that some authors of the included studies considered the 3D CT imaging modality as the gold standard, referring to the study by Bishop et al.⁵⁸ However, Bishop et al. did not validate 3D CT as the gold-standard imaging modality used to perform glenoid bone loss measurement. They concluded that 3D CT is probably the best imaging modality to predict glenoid bone loss without the use of electronic measurement tools that may be present in a viewer—not that 3D CT is the gold standard. Furthermore, several studies referred to an imaging modality as the gold standard. The gold standard is defined as the best available test to measure a parameter under reasonable conditions. The (imaging) modality alone is not the gold standard to measure glenoid bone loss. Combined with a glenoid bone loss—measuring method, it could become the gold standard.

Future studies on the accuracy of measurement methods should clearly state the index and reference tests. Radiography and arthroscopy already have a single method that is used. However, a single method should be chosen as a future standard for 2D CT, 3D CT, 2D MRI, and 3D MRI to increase standardization and the strength of the conclusions drawn after this type of research.⁵⁹ The methods and views on the 2D CT, 3D CT, 2D MRI, and 3D MRI modalities are very similar and seem to produce similar results according to the included studies. Therefore, choosing a method that is easy to perform and does not rely on complex measurement tools may be most convenient. Moreover, a suitable gold standard to measure glenoid bone loss should probably rely on 3D volume measurements instead of 2D measurements because this is probably not influenced by scapular tilt and takes glenoid version and concavity, as well as the location of the defect, into account. Furthermore, the glenoid bone loss—measuring methods may be too simplistic to determine recurrence risk because they do not take into account all the stability factors, but they may be valuable in quickly estimating glenoid bone loss. In addition, a different and more comprehensive approach is needed to create a tool that is able to determine recurrence risk by finding a cutoff value. Preferably, this method would take into account all the factors that determine stability. The strength of this study is that it includes a systematic search and thorough selection process with the goal to find all studies reporting on the accuracy of glenoid bone loss—measuring methods and the influence of a modality on that accuracy.

Limitations

There were some limitations to this systematic review. Owing to the heterogeneity of the reported data, a meta-analysis or quantitative analysis was not feasible.

Therefore, the data presented in this study just offer an overview of the current studies covering this subject. Furthermore, the included studies do not agree on a reference measure as the gold standard, which creates controversy on what is considered an accurate measuring method. The Quality Assessment of Diagnostic Accuracy Studies (QUADAS-2) analyses showed a high number of studies with an unclear risk and a few studies showing a high risk of bias.

Conclusions

Consensus regarding the gold standard in measuring glenoid bone loss is lacking. The use of heterogeneous data and varying methods contributes to differences in the gold standard, and accuracy therefore cannot be determined.

Acknowledgment

The authors thank the clinical librarian F.S. van Etten—Jamaludin for helping them with the search. Furthermore, they thank P.R. Zwanenburg for the illustrations of the bone structures to illustrate the measurement methods.

References

1. Zacchilli MA, Owens BD. Epidemiology of shoulder dislocations presenting to emergency departments in the United States. *J Bone Joint Surg Am* 2010;92:542-549.
2. Shah A, Judge A, Delmestri A, et al. Incidence of shoulder dislocations in the UK, 1995-2015: A population-based cohort study. *BMJ Open* 2017;7:e016112.
3. Hovelius L, Olofsson A, Sandstrom B, et al. Nonoperative treatment of primary anterior shoulder dislocation in patients forty years of age and younger. A prospective twenty-five-year follow-up. *J Bone Joint Surg Am* 2008;90:945-952.
4. Griffith JF, Antonio GE, Yung PS, et al. Prevalence, pattern, and spectrum of glenoid bone loss in anterior shoulder dislocation: CT analysis of 218 patients. *AJR Am J Roentgenol* 2008;190:1247-1254.
5. Porcellini G, Campi F, Paladini P. Arthroscopic approach to acute bony Bankart lesion. *Arthroscopy* 2002;18:764-769.
6. Yiannakopoulos CK, Mataragas E, Antonogiannakis E. A comparison of the spectrum of intra-articular lesions in acute and chronic anterior shoulder instability. *Arthroscopy* 2007;23:985-990.
7. Roberts SB, Beattie N, McNiven ND, Robinson CM. The natural history of primary anterior dislocation of the glenohumeral joint in adolescence. *Bone Joint J* 2015;97-B:520-526.
8. Spatschil A, Landsiedl F, Anderl W, et al. Posttraumatic anterior-inferior instability of the shoulder: Arthroscopic findings and clinical correlations. *Arch Orthop Trauma Surg* 2006;126:217-222.

9. Widjaja AB, Tran A, Bailey M, Proper S. Correlation between Bankart and Hill-Sachs lesions in anterior shoulder dislocation. *ANZ J Surg* 2006;76:436-438.
10. Su F, Kowalczyk M, Ikpe S, Lee H, Sabzevari S, Lin A. Risk factors for failure of arthroscopic revision anterior shoulder stabilization. *J Bone Joint Surg Am* 2018;100:1319-1325.
11. Wiesel BB, Gartsman GM, Press CM, et al. What went wrong and what was done about it: Pitfalls in the treatment of common shoulder surgery. *J Bone Joint Surg Am* 2013;95:2061-2070.
12. Burkhart SS, De Beer JF. Traumatic glenohumeral bone defects and their relationship to failure of arthroscopic Bankart repairs: Significance of the inverted-pear glenoid and the humeral engaging Hill-Sachs lesion. *Arthroscopy* 2000;16:677-694.
13. Zimmermann SM, Scheyerer MJ, Farshad M, Catanzaro S, Rahm S, Gerber C. Long-term restoration of anterior shoulder stability: A retrospective analysis of arthroscopic Bankart repair versus open Latarjet procedure. *J Bone Joint Surg Am* 2016;98:1954-1961.
14. Rollick NC, Ono Y, Kurji HM, et al. Long-term outcomes of the Bankart and Latarjet repairs: A systematic review. *Open Access J Sports Med* 2017;8:97-105.
15. Skupinski J, Piechota MZ, Wawrzyniec W, Maczuch J, Babinska A. The bony Bankart lesion: How to measure the glenoid bone loss. *Pol J Radiol* 2017;82:58-63.
16. Saliken DJ, Bornes TD, Bouliane MJ, Sheps DM, Beaupre LA. Imaging methods for quantifying glenoid and Hill-Sachs bone loss in traumatic instability of the shoulder: A scoping review. *BMC Musculoskelet Disord* 2015;16:164.
17. Sugaya H, Moriishi J, Dohi M, Kon Y, Tsuchiya A. Glenoid rim morphology in recurrent anterior glenohumeral instability. *J Bone Joint Surg Am* 2003;85a:878-884.
18. Itoi E, Lee SB, Amrami KK, Wenger DE, An KN. Quantitative assessment of classic anteroinferior bony Bankart lesions by radiography and computed tomography. *Am J Sports Med* 2003;31:112-118.
19. Yanke AB, Shin JJ, Pearson I, et al. Three-dimensional magnetic resonance imaging quantification of glenoid bone loss is equivalent to 3-dimensional computed tomography quantification: Cadaveric study. *Arthroscopy* 2017;33:709-715.
20. Provencher MT, Detterline AJ, Ghodadra N, et al. Measurement of glenoid bone loss: A comparison of measurement error between 45 degrees and 0 degrees bone loss models and with different posterior arthroscopy portal locations. *Am J Sports Med* 2008;36:1132-1138.
21. Walter WR, Samim M, LaPolla FWZ, Gyftopoulos S. Imaging quantification of glenoid bone loss in patients with glenohumeral instability: A systematic review [published online March 5, 2020]. *AJR Am J Roentgenol*. <https://doi.org/10.2214/AJR.18.20504>.
22. Moher D, Liberati A, Tetzlaff J, Altman DG, PRISMA Group. Preferred reporting items for systematic reviews and meta-analyses: The PRISMA statement. *PLoS Med* 2009;6:e1000097.
23. Poehling GG, Jenkins CB. Levels of evidence and your therapeutic study: What's difference with cohorts, controls, and cases? *Arthroscopy* 2004;20:563.
24. Whiting PF, Rutjes AW, Westwood ME, et al. QUADAS-2: A revised tool for the quality assessment of diagnostic accuracy studies. *Ann Intern Med* 2011;155:529-536.
25. Bakshi NK, Cibulas GA, Sekiya JK, Bedi A. A clinical comparison of linear- and surface area-based methods of measuring glenoid bone loss. *Am J Sports Med* 2018;46:2472-2477.
26. Bakshi NK, Patel I, Jacobson JA, Debski RE, Sekiya JK. Comparison of 3-dimensional computed tomography-based measurement of glenoid bone loss with arthroscopic defect size estimation in patients with anterior shoulder instability. *Arthroscopy* 2015;31:1880-1885.
27. Chuang TY, Adams CR, Burkhart SS. Use of preoperative three-dimensional computed tomography to quantify glenoid bone loss in shoulder instability. *Arthroscopy* 2008;24:376-382.
28. Gyftopoulos S, Beltran LS, Yemin A, et al. Use of 3D MR reconstructions in the evaluation of glenoid bone loss: A clinical study. *Skeletal Radiol* 2014;43:213-218.
29. Gyftopoulos S, Yemin A, Beltran L, Babb J, Bencardino J. Engaging Hill-Sachs lesion: Is there an association between this lesion and findings on MRI? *AJR Am J Roentgenol* 2013;201:W633-W638.
30. Parada SA, Eichinger JK, Dumont GD, et al. Accuracy and reliability of a simple calculation for measuring glenoid bone loss on 3-dimensional computed tomography scans. *Arthroscopy* 2018;34:84-92.
31. Vopat BG, Cai W, Torriani M, et al. Measurement of glenoid bone loss with 3-dimensional magnetic resonance imaging: A matched computed tomography analysis. *Arthroscopy* 2018;34:3141-3147.
32. Lansdown DA, Cvetanovich GL, Verma NN, et al. Automated 3-dimensional magnetic resonance imaging allows for accurate evaluation of glenoid bone loss compared with 3-dimensional computed tomography. *Arthroscopy* 2019;35:734-740.
33. Giles JW, Owens BD, Athwal GS. Estimating glenoid width for instability-related bone loss: A CT evaluation of an MRI formula. *Am J Sports Med* 2015;43:1726-1730.
34. Rouleau DM, Garant-Saine L, Canet F, Sandman E, Menard J, Clement J. Measurement of combined glenoid and Hill-Sachs lesions in anterior shoulder instability. *Shoulder Elbow* 2017;9:160-168.
35. Stillwater L, Koenig J, Maycher B, Davidson M. 3D-MR vs. 3D-CT of the shoulder in patients with glenohumeral instability. *Skeletal Radiol* 2017;46:325-331.
36. Griffith JF, Yung PS, Antonio GE, Tsang PH, Ahuja AT, Chan KM. CT compared with arthroscopy in quantifying glenoid bone loss. *AJR Am J Roentgenol* 2007;189:1490-1493.
37. Lee RK, Griffith JF, Tong MM, Sharma N, Yung P. Glenoid bone loss: Assessment with MR imaging. *Radiology* 2013;267:496-502.
38. Tian CY, Shang Y, Zheng ZZ. Glenoid bone lesions: Comparison between 3D VIBE images in MR arthrography and nonarthrographic MSCT. *J Magn Reson Imaging* 2012;36:231-236.
39. Magarelli N, Milano G, Baudi P, et al. Comparison between 2D and 3D computed tomography evaluation of glenoid bone defect in unilateral anterior gleno-humeral instability. *Radiol Med* 2012;117:102-111.

40. Stecco A, Guenzi E, Cascone T, et al. MRI can assess glenoid bone loss after shoulder luxation: Inter- and intra-individual comparison with CT. *Radiol Med* 2013;118:1335-1343.
41. Miyatake K, Takeda Y, Fujii K, Takasago T, Iwame T. Validity of arthroscopic measurement of glenoid bone loss using the bare spot. *Open Access J Sports Med* 2014;5:37-42.
42. Murachovsky J, Bueno RS, Nascimento LG, et al. Calculating anterior glenoid bone loss using the Bernageau profile view. *Skeletal Radiol* 2012;41:1231-1237.
43. Souza PME, Brandao BL, Brown E, Motta G, Monteiro M, Marchiori E. Recurrent anterior glenohumeral instability: The quantification of glenoid bone loss using magnetic resonance imaging. *Skeletal Radiol* 2014;43:1085-1092.
44. Lacheta L, Herbst E, Voss A, et al. Insufficient consensus regarding circle size and bone loss width using the ratio-"best fit circle"-method even with three-dimensional computed tomography. *Knee Surg Sports Traumatol Arthrosc* 2019;27:3222-3229.
45. Pansard E, Klouche S, Billot N, et al. Reliability and validity assessment of a glenoid bone loss measurement using the Bernageau profile view in chronic anterior shoulder instability. *J Shoulder Elbow Surg* 2013;22:1193-1198.
46. Shin SJ, Kim RG, Jeon YS, Kwon TH. Critical value of anterior glenoid bone loss that leads to recurrent glenohumeral instability after arthroscopic Bankart repair. *Am J Sports Med* 2017;45:1975-1981.
47. Lee JH, Park JS, Hwang HJ, Jeong WK. Time to peak torque and acceleration time are altered in male patients following traumatic shoulder instability. *J Shoulder Elbow Surg* 2018;27:1505-1511.
48. Locher J, Wilken F, Beitzel K, et al. Hill-Sachs off-track lesions as risk factor for recurrence of instability after arthroscopic Bankart repair. *Arthroscopy* 2016;32:1993-1999.
49. Verweij LPE, van Deurzen DFP, Kerkhoffs G, van den Bekerom MPJ. A clinical comparison of linear- and surface area-based methods of measuring glenoid bone loss: Letter to the editor. *Am J Sports Med* 2019;47:NP28-NP29 (letter).
50. Haas M, Plachel F, Wierer G, et al. Glenoid morphology is associated with the development of instability arthropathy. *J Shoulder Elbow Surg* 2019;28:893-899.
51. Griffin JW, Collins M, Leroux TS, et al. The influence of bone loss on glenoid version measurement: A computer-modeled cadaveric analysis. *Arthroscopy* 2018;34:2319-2323.
52. Moroder P, Ernstbrunner L, Pomwenger W, et al. Anterior shoulder instability is associated with an underlying deficiency of the bony glenoid concavity. *Arthroscopy* 2015;31:1223-1231.
53. Moroder P, Plachel F, Huettnner A, et al. The effect of scapula tilt and best-fit circle placement when measuring glenoid bone loss in shoulder instability patients. *Arthroscopy* 2018;34:398-404.
54. Saito H, Itoi E, Sugaya H, Minagawa H, Yamamoto N, Tuoheti Y. Location of the glenoid defect in shoulders with recurrent anterior dislocation. *Am J Sports Med* 2005;33:889-893.
55. Lansdown DA, Wang K, Bernardoni E, et al. Variability in the contour of cadaveric anterior and posterior glenoids based on ipsilateral 3-dimensional computed tomography reconstructions: Implications for clinical estimation of bone loss. *Arthroscopy* 2018;34:2560-2566.
56. Barcia AM, Rowles DJ, Bottoni CR, Dekker TJ, Tokish JM. Glenoid bare area: Arthroscopic characterization and its implications on measurement of bone loss. *Arthroscopy* 2013;29:1671-1675.
57. Kralinger F, Aigner F, Longato S, Rieger M, Wambacher M. Is the bare spot a consistent landmark for shoulder arthroscopy? A study of 20 embalmed glenoids with 3-dimensional computed tomographic reconstruction. *Arthroscopy* 2006;22:428-432.
58. Bishop JY, Jones GL, Rerko MA, Donaldson C, MOON Shoulder Group. 3-D CT is the most reliable imaging modality when quantifying glenoid bone loss. *Clin Orthop Relat Res* 2013;471:1251-1256.
59. Teske LG, Waterman BR. Editorial Commentary: Shoulder bone loss for dummies: A reproducible technique for quantifying glenohumeral osseous defects. *Arthroscopy* 2019;35:1794-1795.

Appendix Table 1. PubMed (MEDLINE) Search Terms

(((((("Glenoid Cavity"[Mesh] OR gleno*[tiab] OR "Humeral Head"[Mesh] OR humer*[tiab]) AND (loss[tiab] OR defect*[tiab]))) OR ((bony[tiab] OR osseous[tiab]) AND ("Bankart Lesions"[Mesh] OR bankart[tiab] OR (Hill[tiab] AND Sachs[tiab])))) AND (("Diagnostic Imaging"[Mesh] OR "Radiography"[Mesh] OR "diagnostic imaging" [Subheading] OR imaging[tiab] OR CT[tiab] OR MRI[tiab] OR magnetic resonance imaging*[tiab] OR computed tomograph*[tiab] OR radiography[tiab] OR x-ray*[tiab])) AND (english[Language] OR dutch[Language] OR german[Language] OR french[Language]) AND ("1994/01/01"[Date - Publication] : "3000"[Date - Publication]))

Appendix Table 3. Cochrane Database Search Terms

No.	Search
1	(gleno* or humer*) and (loss or defect*):ti,ab,kw (Word variations have been searched)
2	(bony or osseous) and (bankart):ti,ab,kw (Word variations have been searched)
3	(bony or osseous) and (Hill and Sachs):ti,ab,kw (Word variations have been searched)
4	1 or 2 or 3
5	MeSH descriptor: [Diagnostic Imaging] explode all trees
6	MeSH descriptor: [Radiography] explode all trees
7	imaging or CT or MRI or magnetic resonance imaging* or computed tomograph* or radiography or x-ray*:ti,ab,kw (Word variations have been searched)
8	5 or 6 or 7
9	4 and 8 Publication Year from 1994 to 2019

Appendix Table 2. Embase Search Terms

No.	Search
1	(glenoid cavity/ or humeral head/ or (gleno* or humer*).ti,ab,kw.) and (loss or defect*).ti,ab,kw.
2	((bony or osseous) and (bankart or (Hill and Sachs))).ti,ab,kw.
3	(bony or osseous).ti,ab,kw. and Bankart lesion/
4	1 or 2 or 3
5	diagnostic imaging/ or radiography/ or bone radiography/ or exp joint radiography/
6	(imaging or CT or MRI or magnetic resonance imaging* or computed tomograph* or radiography or x-ray*).ti,ab,kw.
7	5 or 6
8	4 and 7
9	limit 8 to (dutch or english or french or german)
10	limit 9 to yr="1994 -Current"